Journal of Geosciences and Geomatics, 2021, Vol. 9, No. 2, 45-54
Available online at http://pubs.sciepub.com/jgg/9/2/1
Published by Science and Education Publishing
DOI:10.12691/jgg-9-2-1

Contribution of Gravity and Hydrogeological Implication to the Study of the Subsoil in the East Region (Cameroon)

Edouard Olivier Ntomb Biboum[1,2,*], Sterve Alain Lepatio Tchieg[2,3], Estelle Eric Fosso Téguia M.[1,4], Vanessa Gaelle Nana[1,2], Rachel Ngo Nyouma[2,5], Henri Emile Pougue Eone[1], Ntepe Nfomou[1]

[1]Branch for Geophysical and Volcanological Research / Institute for Geological and Mining Research, P. O. Box 370 Buea, Cameroon
[2]University of Yaoundé 1, faculty of science, department of physics, P. O. Box 812 Yaoundé, Cameroon
[3]National Institute of Cartography, P. O. Box 157 Yaoundé, Cameroon
[4]Institute of Geosciences, Kiel University, Kiel, Germany
[5]Ore processing Laboratry/Institute for Geological and Mining Research, P. O. Box 4110 Yaoundé, Cameroon
*Corresponding author: edouardbibs@yahoo.fr

Received April 14, 2021; Revised May 17, 2021; Accepted May 27, 2021

Abstract A geophysical study combining gravimetric and geo-electric methods was carried out in East Cameroon in order to characterize the soil and subsoil of this area. This work constitutes a preliminary study for the evaluation of areas suitable for hydraulic drilling. The aim of this work is to determine the different lineaments that would be found in this area as well as the different layers of land found in this part of Cameroon. The superposition of maxima map of the horizontal gradient reveals the presence of E-W, N-S, ENE-WSW, NNW-SSE, NNE-SSW and NE-SW oriented contacts. Borings curves obtained from the geoelectrical data allowed the geological section of the area to be drawn up, which is characterized by laterites, clays and fissured granites.

Keywords: *gravity, geo-electricity, bouguer anomaly, resistivity, lineaments*

Cite This Article: Edouard Olivier Ntomb Biboum, Sterve Alain Lepatio Tchieg, Estelle Eric Fosso Téguia M., Vanessa Gaelle Nana, Rachel Ngo Nyouma, Henri Emile Pougue Eone, and Ntepe Nfomou, “Contribution of Gravity and Hydrogeological Implication to the Study of the Subsoil in the East Region (Cameroon).” *Journal of Geosciences and Geomatics*, vol. 9, no. 2 (2021): 45-54. doi: 10.12691/jgg-9-2-1.

1. Introduction

Methods based on potential fields have been widely used for many years to map anomalies due to specific contrasts in the earth's crust. Gravimetry is used to highlight areas of the subsurface with a density contrast. The boundaries between these zones are detected by analyzing the gravimetric gradients [1,2,3,4]. Our study area is located in the eastern part of Cameroon and is affected by a series of tectonic accidents due to the collision between the Pan-African chain and the Congo craton [5,6,7,8,9]. This area has already been the subject of several studies. The results of [10] revealed that the Lower Eseka-Dja fault line is located in the granitic basement of the Ntem complex slightly south of the granite/chist metamorphic contact that constitutes the overthrust line to the Congo craton. The work of [11] suggests an E-W normal fault in the Mengueme-Abong-Mbang area; while [12] highlight areas of high gravity gradients that separate different anomalies. A geoelectrical investigation was carried out in the Batouri area to highlight the presence of clay minerals in the Tindikala-Boutou area along the Kadey River using the continuous flow method. The study identified a large conductive weakness or discontinuity as a Precambrian granitic shear zone in agreement with previous geological and tectonic studies [13]. Another geoelectrical investigation had been carried out in the same Tindikala-Boutou area aiming to identify host structures for gold mineralization by direct current and induced polarization methods [14].

The geomorphology of the area makes groundwater exploration difficult, thus limiting access to groundwater resources. In this work, we propose to conduct a soil and subsoil reconnaissance study for the feasibility of hydraulic drilling. The gravimetric results will highlight the existence of lineaments in the area, which would constitute real traps for the aquifers. The electrical method revealed the different layers of soil present in the area.

2. Geological Setting

The entire Eastern Region of Cameroon is made up of older land forming the old Precambrian basement (Figure 1). Folded metamorphic rocks and several series of intrusive granites can be distinguished. There are also non-metamorphic sedimentary terrains. A boring on the Boden-Batouri road revealed the presence of gravels whose appearance is characteristic of the features of the horizontal sandstones of the Oubangui. A little further south, about 100 km along the Mdokayo-Batouri track, horizontal sandstones of the Carnot Sandstone series were observed [15]. Geological surveys conducted in recent years [16-21] reveal that Central Africa consists of a Precambrian basement. [22] show that the Eastern Region is underlain by an old basement of Precambrian age.

The tectonics of East Cameroon indicate that this part of the country corresponds to the mobile zone of Central Africa, where the Pan-African orogeny took place. This orogenic zone affects the majority of the metamorphic terrains of Central Africa and occupies almost all of Cameroon. The most abundant rocks are granites and migmatites.

Geochronological work [24] allows the evolution of the northern edge of the Congo Craton during the Archean and Proterozoic to be related to major tectonic episodes. The Proterozoic cover of the craton is framed by two breakaway zones that characterize three blocks [25]. The Pan-African chain is considered to be the result of convergence and collision between the Congo Craton and the mobile belt [6,8,18,26,27,28,29,30], or as a collision between different blocks of the mobile belt [7,31].

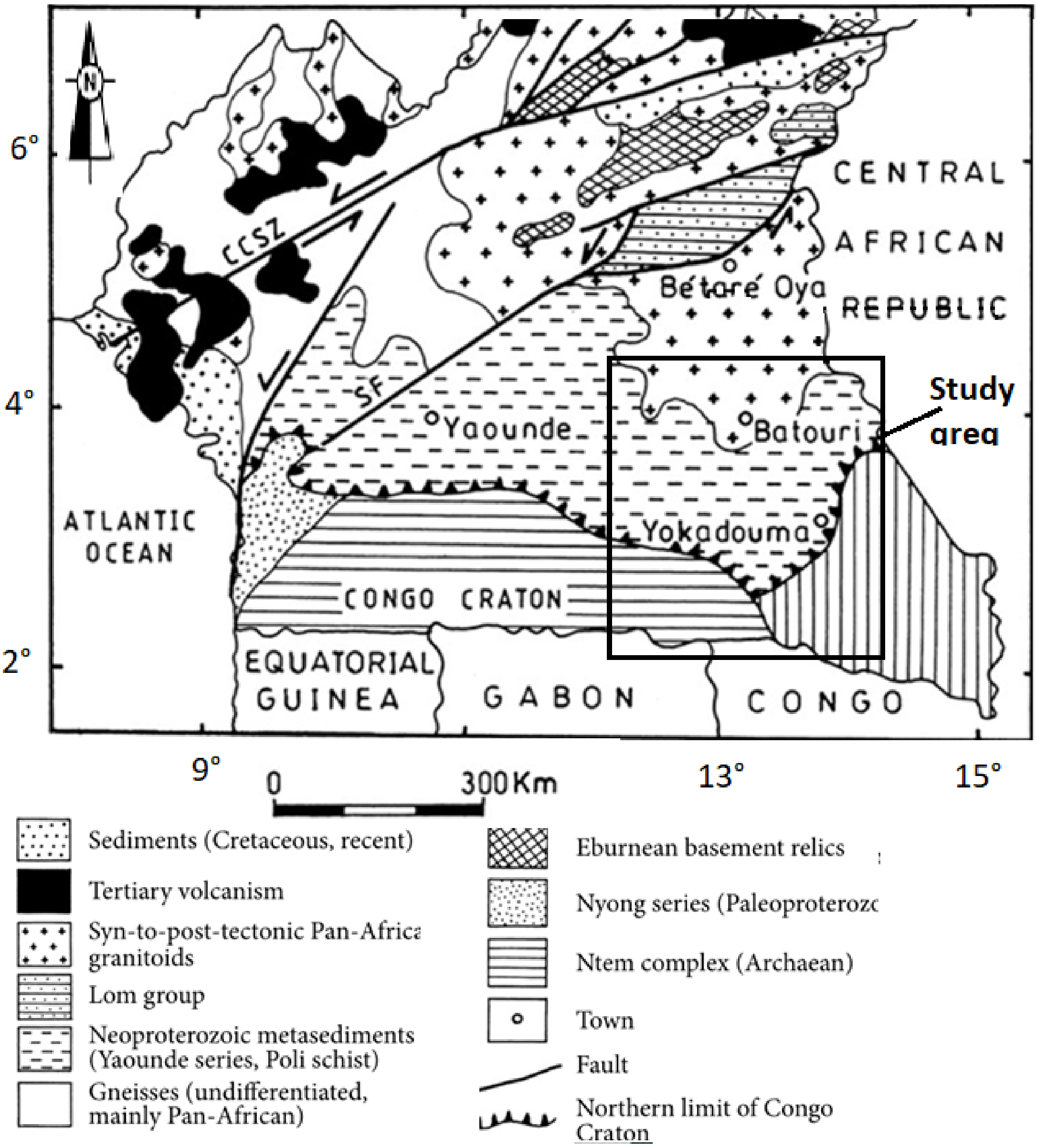

Figure 1. Geological map of the study area modified from [23]

3. Data and Processing

3.1. Gravity

This work was made possible by using regional Bouguer and free-air gravity anomaly grid data derived from the Earth Gravity Model -EGM2008 [32]. The EGM2008 model has been corrected for long wavelengths (300 km) using data from the GRACE satellite. The model provides local Earth gravity data sets and has proven useful for regional geophysical modelling [33]. This new model provides gravity data with a nominal resolution of 5°x 5°. [34] discussed the EGM2008 model in comparison to field data. The EGM2008 gravity data for the study area was employed to develop the Bouguer anomaly map (Figure 2) using Geosoft software. This map is the result of superimposing the effects of geological structures located at varying depths (shallow, medium and deep). It also contains information on discontinuities in the subsurface.

The Bouguer anomaly map obtained shows all negative anomaly values, with amplitudes ranging from -109.9 à -35.2 mGal, and reflects the lateral variations of the density in the subsurface. There are two areas of low anomaly, one in the north and the other in the west. In the north, there is a sector of light anomalies with a main E-W direction. This anomaly could correspond to an intrusion of light rocks such as granites. The light anomalies, very localized, would characterize small sedimentary basins which are most often structures related to subsidence. The medium anomalies with a closed contour cover the southern part of the map with an amplitude ranging from -87.3 à -78.5 mGal. The heavy anomalies with a general WNW-ESE direction and an amplitude ranging from -70.5 à -35.2 mGal, are much more observed in the center of the Bouguer anomaly map covering the localities of Minta, Bertoua, Batouri, Abong Mbang and Yokadouma. These anomalies may be associated with either basement uplift, or intrusions of high-density rocks or heavy material deposits in the basement. The gradients observed in the study area materialize discontinuities or transitions between heavy and light gravity sectors. These gradient zones are formed as elongated bands.

The residual anomaly map is obtained by subtracting the regional anomaly from the Bouguer anomaly. Recall that the regional map chosen for this work is the Bouguer map extended upwards to 10 km since we are interested in the effects of surface structures.

Figure 3 shows the positive and negative anomalies related to the anomalies observed on the Bouguer map. However, there is a large discrepancy with the Bouguer anomaly map in some places, reflecting the deformation of the basement.

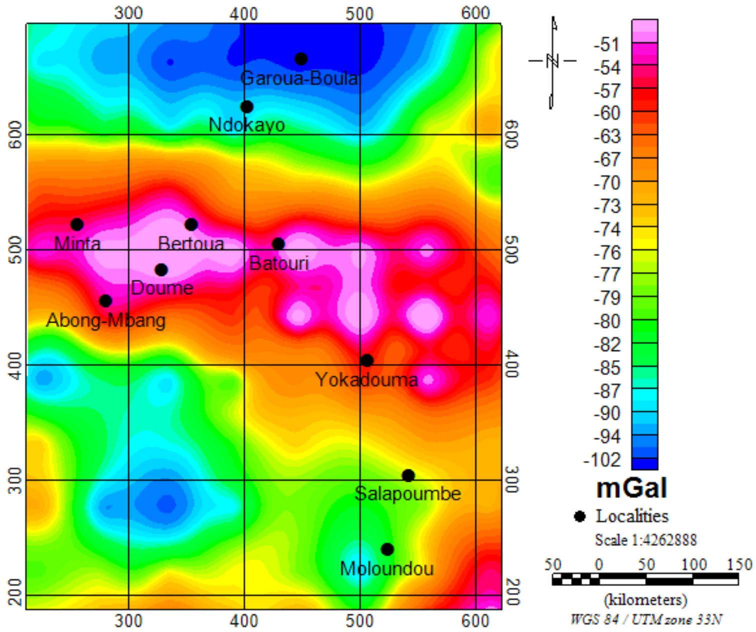

Figure 2. Bouguer anomaly map of the study area

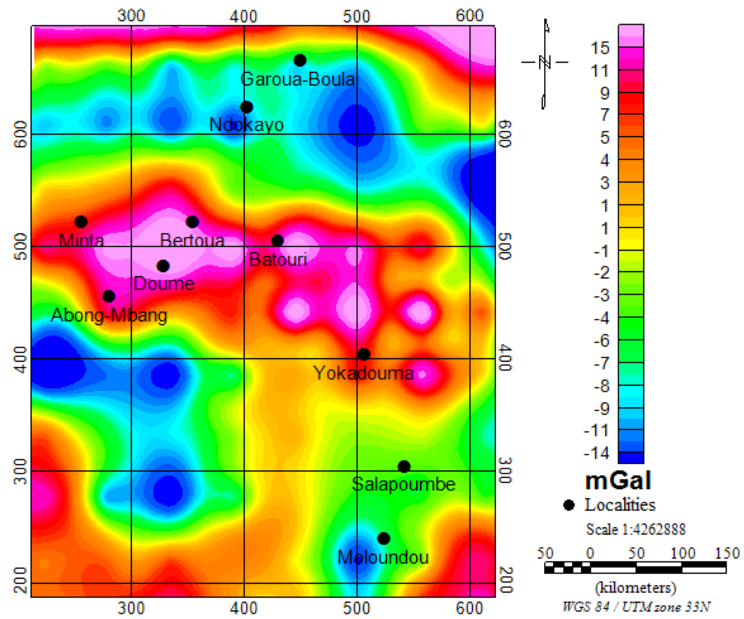

Figure 3. Residual anomaly map

This residual anomaly map illustrates individualized positive and negative anomalies which appear at a depth of 1500 m, with an amplitude between -21.0 and 31.3 mGal and are separated by gradient zones.

The light residual anomalies observed on the residual anomaly map (Figure 3), are located to the north, northwest, east and west with amplitudes ranging from -21.0 à -9.4 mGal. They are due to a bowl-shaped formation and suggest subsidence or a trough-giving rise to a thickening of the ground. The heavy residual anomaly zones are three in number, characterized by positive residual anomalies, one of which predominates in the center of the map covering Minta, Bertoua, Batouri, Abong Mbang and Yokadouma with a WNW-ESE direction and an amplitude from 5,9 to 31,3 mGal. It can be interpreted as an intrusion of very dense material whose nature remains to be determined. The separation corridors of the negative and positive anomalies are likely to be fault zones or tectonic faults.

The vertical gradient map highlights anomalies with low amplitudes and short wavelengths. The vertical gradient is used to amplify short-wavelength anomalies and individualize bodies [35]. Figure 4 shows the vertical gradient map of residual anomalies with amplitudes ranging from -5.3E-04 to 5.6E-03 mGal/m. We note on this map that the heavy anomalies correspond to the granites and migmatites outcropping on the surface. The light anomalies on this map are scattered throughout the map and can be associated with synformal structures. These group of anomalies contain values ranging from -5.3E-04 to -2.1E-04 mGal/m.

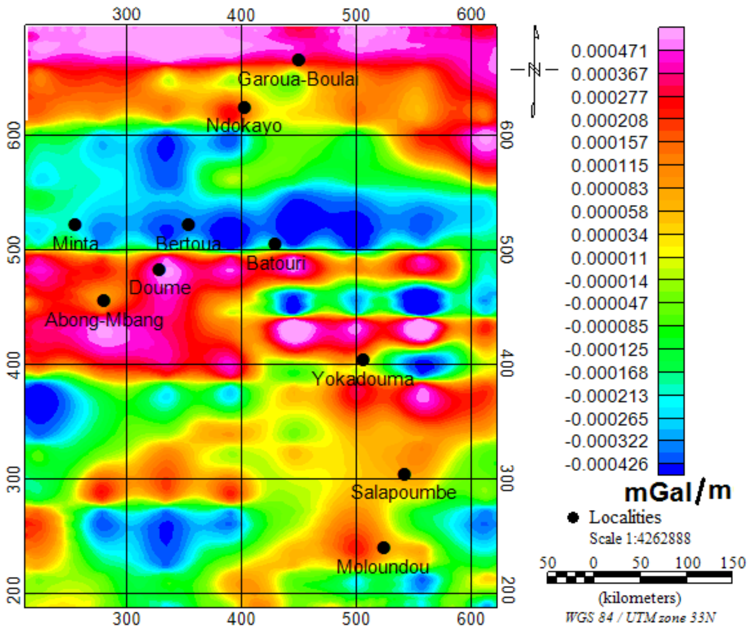

Figure 4. Vertical gradient map of the study area

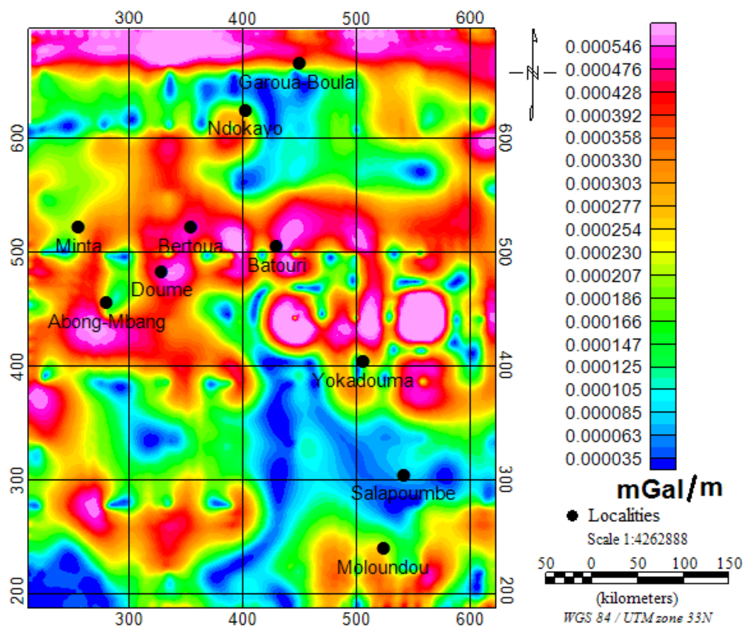

Figure 5. Horizontal gradient map of the Bouguer anomaly

Gravity plays an important role in the identification of deep faults, their boundaries and branching [36,37,38,39]. The horizontal gradient map (Figure 5) of the Bouguer Anomaly shows a priori almost equally distributed gradient zones. Considering a gravity feld $G(x,y)$, the horizontal gradient magnitude HG is giving by the following expression (equation 1) [40].

$$HG = \sqrt{\left(\frac{\partial G(x,y)}{\partial x}\right)^2 + \left(\frac{\partial G(x,y)}{\partial y}\right)^2} \quad (1)$$

It shows areas of horizontal gradients with almost circular amplitudes and shapes. On the map, it is easy to distinguish the gradient zones corresponding to contact/fault type structures (high gradient zone) and those corresponding to the presence of intrusive formations.

In the center and far north of the study area, we note the presence of strong horizontal gradients, i.e. high densities (≥3.58E-04 mGal/m) are observed along the S-N direction. They indicate a major tectonic structure penetrating the crust. This structure would have been favored by the collapse of the region's basement.

Figure 6 shows local maxima of the horizontal gradient extended upwards at several altitudes, including 0 m to 10 km. According to [38], this superposition of maxima allows the geological contacts associated with the faults or fractures suspected in the previous maps to be highlighted. The degree of importance (depth) of a lineament is determined by the continuous presence of local maxima at increasingly higher elevations of the upward extension. Analysis of the maxima of the horizontal gradient of the Bouguer Anomaly extended upwards at these different altitudes shows precisely the orientation of the dip of each lineament.

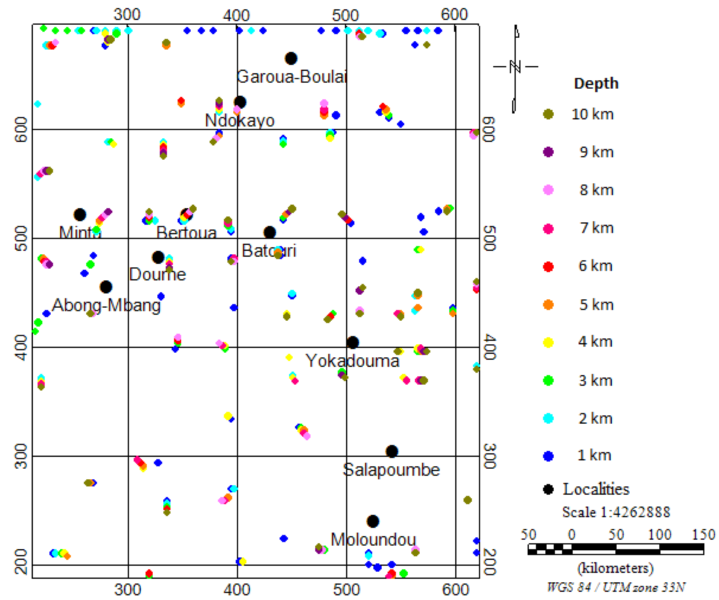

Figure 6. Superposition map of horizontal gradient maxima

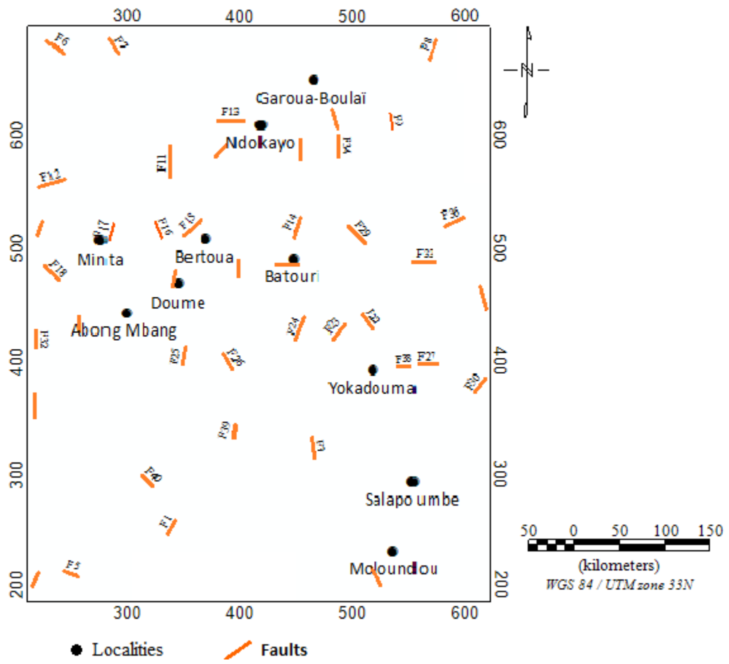

Figure 7. Interpretative structural map of the study area

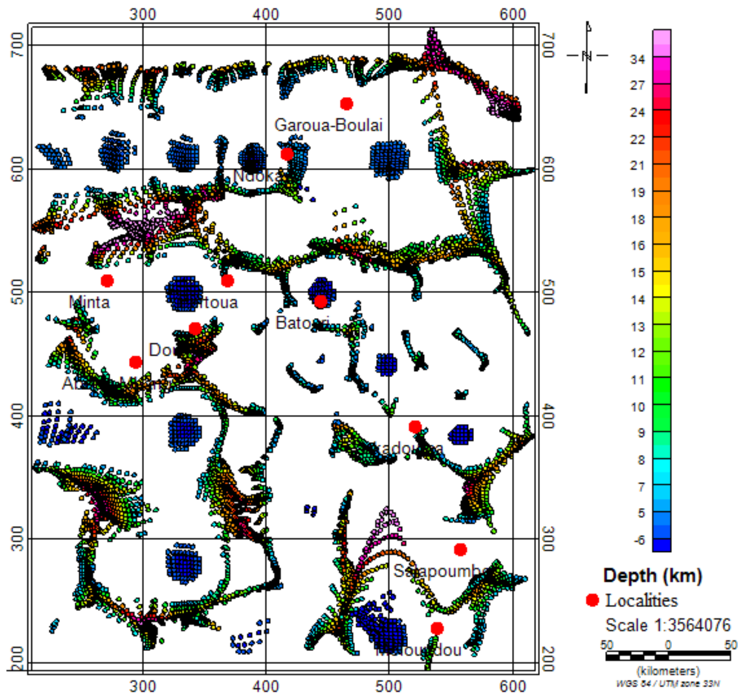

Figure 8. Euler solution map

The lineament map (Figure 7) is obtained by plotting the lineaments resulting from the superposition of the horizontal gradient maxima (Figure 6). These lineaments follow several structural directions including: E-W, N-S, ENE-WSW, NNW-SSE, NNE-SSW and NE-SW.

The results obtained from the processing of the gravity anomalies confirm and clarify the arrangement of the brittle structures recognized by the geological studies, and highlight new lineaments. The lineaments on the upwardly extended horizontal gradient map correspond to the major features affecting the study area.

The interpretative structural map (Figure 8) shows that the fractures are dense and oriented in almost all directions. The more fractured the area is, the more interconnected the fractures are and the higher the chance of encountering a productive fracture. The strong presence of tectonic lineaments in the study area facilitates the preferential circulation of groundwater, which may imply the presence of abundant fractured aquifers.

3.2. Electrical method

The geoelectrical data used in this study were collected in 2013 by GEOFOR Constructions S.A., a company specializing in geotechnical and hydraulic drilling. Six electrical boreholes were carried out in our study area as shown in Table 1. The maximum spacing of the injection electrodes is 166 m, which corresponds to an average borehole depth of 31.54 m. The data obtained in the field was processed for soil characterization.

The grouping of the curve types allows a first approach to analyze the data, to position the main limits between the different hydrogeological sequences. A different symbol was assigned to each type of electrical curve (A, H, K, Q, KH and many other combinations depending on the number of layers).

In our study area, six electrical sounding curves were made using the JOINTEM software. The interpretation of these curves allowed us to propose a succession of geological layers that is, as close as possible to the geophysical measurements made in the field.

The analysis of the sampling curves (Figure 9) allows us to distinguish five types of curves with Root Mean Square (RMS) between 0.009 and 0.101. These different types of curve are classified in Table 2. The interpretation of the sounding curves highlights the presence of 4 to 5 soil layers. We distinguish between a superficial arable land, laterite, clays which are sandy and lateritic, fractured granites and granites. The following table gives the summary results of the apparent resistivity, the thickness and the types of rock encountered at each depth.

Table 1. Measurement stations and resistivity range

Measuring stations	Longitude (degree)	Latitude (degree)	Altitude (m)	Resistivity (Ω.m)
S1 : Garoua-Boulaï	14,55	5,88	996	[112,1-509,7]
S2 : Minta	12,83	4,56	696	[150,9-829,6]
S3 : Salapoumbe	15,69	2,61	493	[225,7-976,3]
S4 : Moloundou	15,18	2,06	372	[245,7-1129,4]
S5: Yokadouma	15,07	3,53	528	[1129-2155,3]
S6: Abong Mbang	13,17	3,99	694	[251,2-590,1]

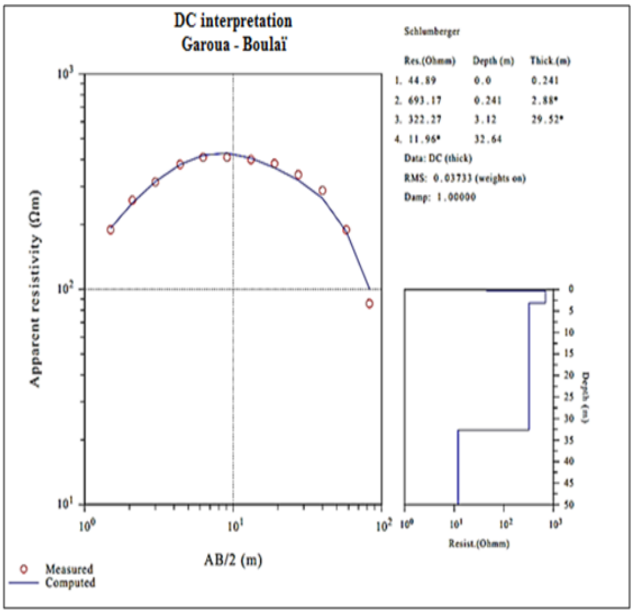

(a) Electrical sounding curve at Garoua – Boulaï station.

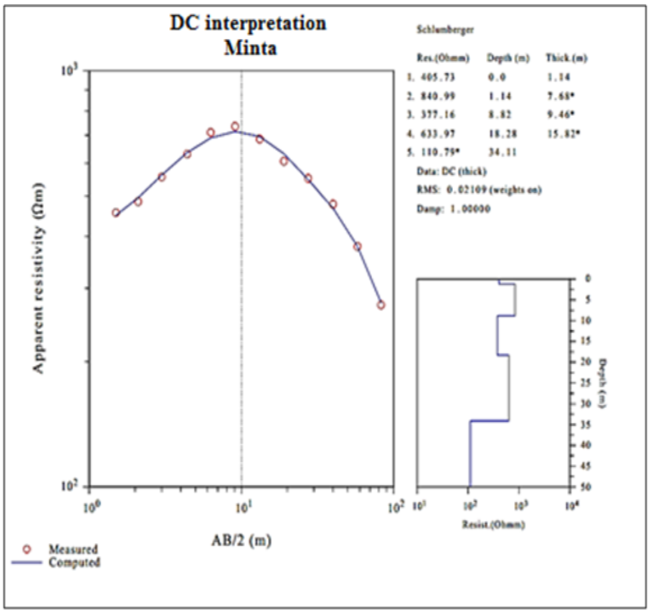

(b) Electrical sounding curve at Minta station

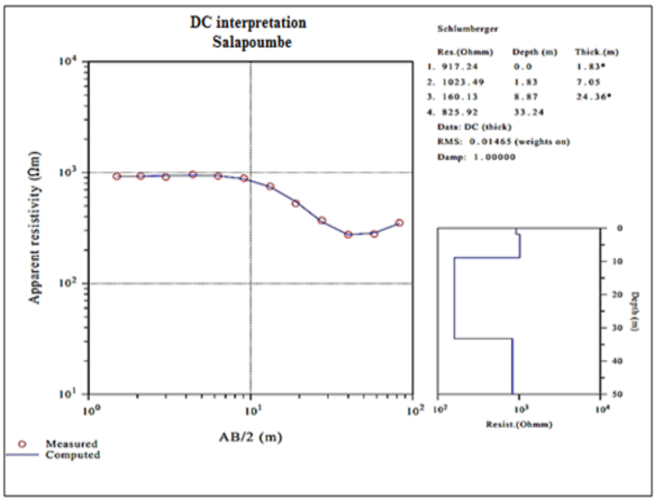

(c) Electrical sounding curve at the Salapoumbe station

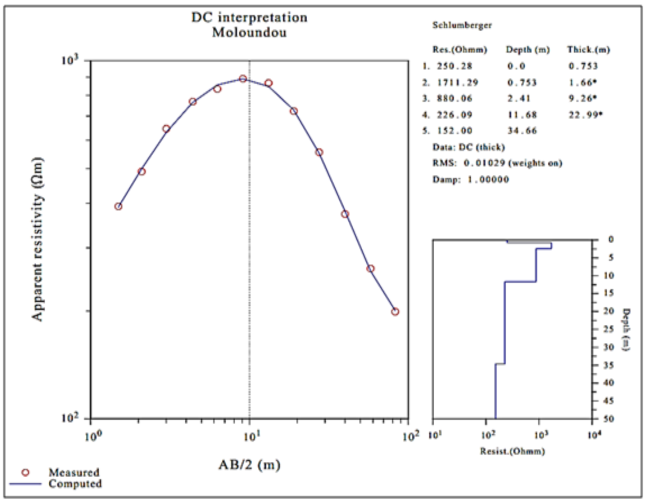

(d) Electrical sounding curve at the Moloundou station.

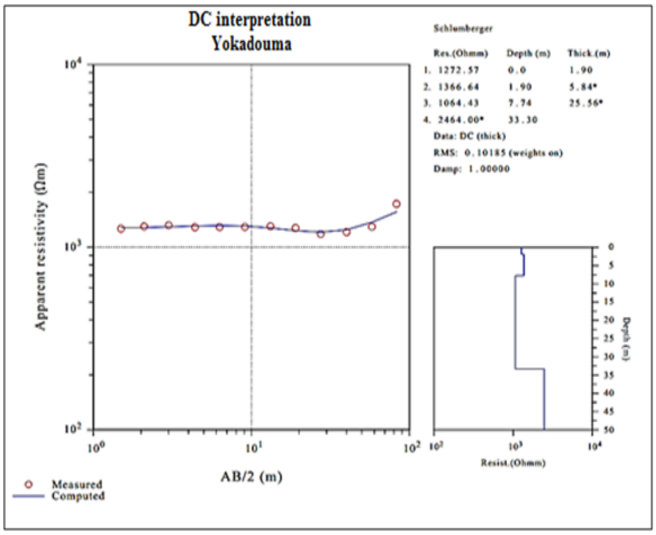

(e) Electrical sounding curve at the Yokadouma station.

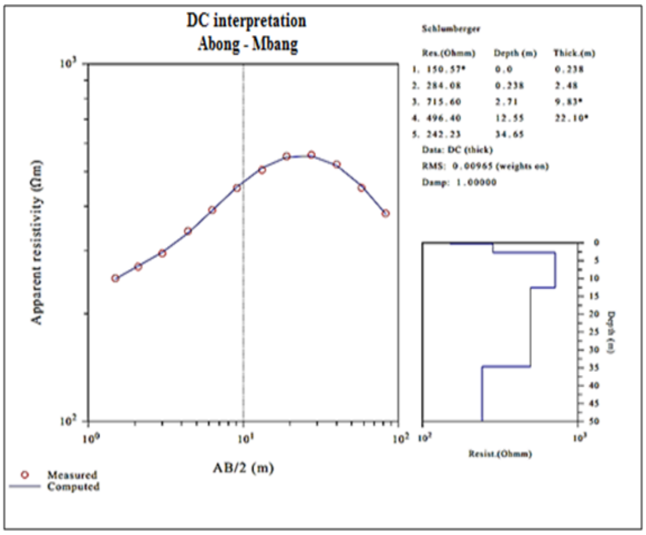

(f) Electrical sounding curve at Abong - Mbang station

Figure 9. Electrical sounding curve at the (a) Garoua-Boulaï, (b) Minta, (c) Salapoumbe, (d) Moloundou, (e) Yokadouma and (f) Abong-Mbang stations

Table 2. Summary table of the different electrical sounding curves in our study area

Stations	Resistivity in Ω.m $\rho_1, \rho_2, \ldots, \rho_n$	Type of curves	Number of Layers	Thickness in (m) $h_1, h_2, \ldots, h_{n-1}$	Total thickness (m)	Type of rock
S1	44,89/693,17/322,27/11,96	KQ	4	0,24/2,88/29,52	32,6	Arable ground/lateritic clay/weathered clay/fractured granite
S2	405,73/840,99/377,16/633,97/110,79	KHK	5	1,14/7,68/9,46/15,82	34,11	Arable ground/laterite, clay/lateritic clay/fractured granite
S3	917,24/1023,49/160,13/825,92	KH	4	1,83/7,05/24,36	33,24	Arable ground/lateritic clay/fractured granite/granite
S4	250,28/1711,29/880,0/226,09/152	KQQ	5	0,75/1,66/9,26/22,99	34,66	Arable ground/laterite/clay/sandy clay/fractured granite
S5	1272,57/1366,64/1064,43/2464	KH	4	1,90/5,84/25,56	33,30	Arable ground /laterite/lateritic clay/granite
S6	150,57/284,08/715,60/469,40/242,23	AKQ	5	0,23/2,48/9,83/22,10	34,65	Arable ground/laterite/weathered lateritic clay/sandy clay/fractured granite

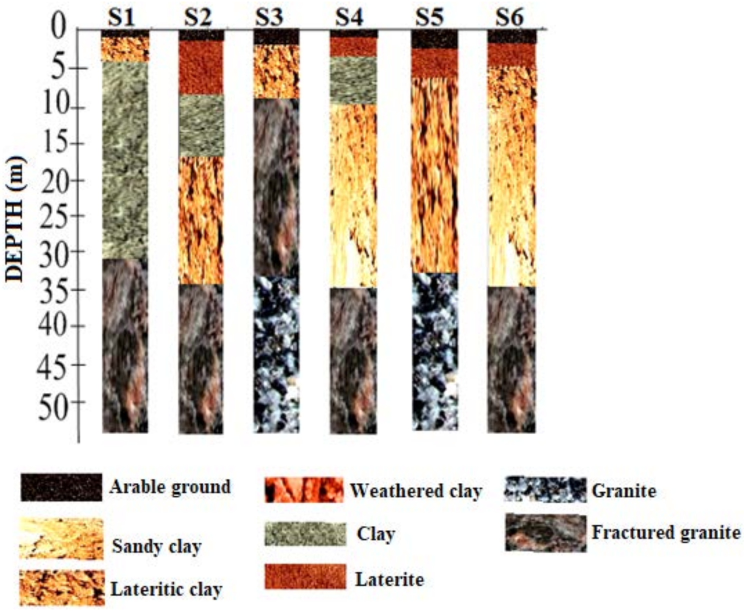

Figure 10. Geological section of the six electrical boring of the study area

The interpretation of the borehole curves allows us to establish the geological section of our study area. This section is obtained from the geoelectric model of the electrical boreholes and the knowledge of the geology of the area. It highlights the geological structure of the subsoil in a vertical direction as shown in Figure 10.

Figure 10 allows us to distinguish a granitic basement with two (02) different geological structures encountered from the surface to the depth and to establish the lithology of this area. To this end, we have subdivided the subsoil of the study area into three layers, as shown in Table 3.

Table 3. Characteristics of the three main subsoil layers in the study area

Number of Layer	Dominant lithology	Resistivity range in (Ω.m)	Thickness range in (m)
1	Arable ground	[44,89-1272,57]	[0,23-1,90]
2	Clay	[226,06-1711,29]	[1,66-29,52]
3	Fractured and fissured granite	[11,96-2464]	Infinity

4. Conclusion

The aim of this study was to obtain knowledge of the subsoil of the East region of Cameroon in order to carry out hydraulic drilling. The results obtained in the framework of this study, after interpretation of the gravity and geoelectric data, provided new elements in terms of knowledge of the structures of the area, confirmation of the presence of certain faults as well as the identification of the ground layers in the study area. The qualitative analysis of the Bouguer anomaly map, indicates that the heavy anomaly zones observed on it with a maximum amplitude of -35.2 mGal are due to intrusions of very high density material in the subsoil. Further analysis has shown that this material is granite. The areas of negative anomalies observed on the map with amplitudes ranging from -87.3 à -78.5 mGal are related to the gravimetric effect of the intrusion of light granites with a negative density contrast to the crust. This granitic intrusion is probably responsible for the large anomaly observed to the north and west of the region and is a consequence of the collapse of the region's basement. The interpretation of the residual anomaly map also permit the researchers to relate it to a number of geological structures already observed at surface level. It equally illustrates on the one hand the close relationship between the light anomalies and collapse of basement and on the other hand the close relationship between the heavy anomalies observed and basement uplift. The analysis of the structural map of the area demonstrates the relatively shallow geological structures of little lateral extension which extend, according to the areas of the study zone, in the following directions: E-W, N-S, ENE-WSW, NNW-SSE, NNE-

SSW and NE-SW. These main tectonic faults responsible for the structuring of the study area are highlighted and well located by the multi-scale analysis of horizontal gravity gradients. The vertical electrical boreholes carried out in our study area allowed us to distinguish a granitic basement with two different geological structures encountered from the surface to the depth and to establish the lithology of this area. The subsoil of the study area was divided into three main layers: arable land, clay and fractured and fissured granites.

Acknowledgements

Authors are grateful to Cameroon Institute for Geological and Mining Research (IRGM) and the Department of Physics, Faculty of Sciences of the University of Yaoundé 1 for providing a framework for this study and to the BGI (Bureau Gravimétrique International) for their kind collaboration by providing EGM2008 data used in this work.

References

[1] Archibald, N., Gow, P., and Boschetti, F., 1999. Multiscale edge analysis of potential field data. Exploration Geophysics, 30, 38-44.

[2] Keating, P., et al., 2004. Locating magnetic contacts and source characteristics from magnetic data: application to the Canadian shield [online]. In: EAGE 66th conference & exhibition, 7-10 June, Paris. Available from: http://earthdoc.eage.org/publication/publicationdetails/?publication=2035.

[3] Khattach, D., et al., 2004. Apport de la gravimétrie à l'étude de la structure du bassin des Triffa (Maroc nord-oriental): implications hydrogéologiques. *Comptes Rendus Geoscience*, 336, 1427-1432.

[4] Khattach, D., et al., 2006. Analyse multi-échelle par ondelettes des contacts géologiques : application à la carte gravimétrique du Maroc nord-oriental. *Comptes Rendus Geoscience*, 338, 521-526.

[5] Nzenti, J.-P., Barbey, P., Jegouzo, P., et al. Un nouvel exemple de ceinture granulitique dans une chaîne protézoïque de collision: les migmatites de Yaoundé au Cameroun. Comptes-rendus des séances de l'Académie des sciences. Série 2, Mécanique-physique, chimie, sciences de l'univers, sciences de la terre. 299(17) (1984), 1197-1199.

[6] Nzenti, J. P., Barbey, P., Macaudiere, J., et al. Origin and evolution of the late Precambrian high-grade Yaounde gneisses (Cameroon). *Precambrian research*, 38(2) (1988) 91-109.

[7] Castaing, C., Feybesse, J. L., Thiéblemont, D., et al. Palaeogeographical reconstructions of the Pan-African/Brasiliano orogen: closure of an oceanic domain or intracontinental convergence between major blocks. *Precambrian Research*, 69(1-4) (1994), 327-344.

[8] Abdelsalam, Mohamed G., Liégeois, Jean-Paul, and Stern, Robert J. The saharan metacraton. *Journal of African Earth Sciences*, 34(3-4) (2002), 119-136.

[9] Toteu, S.F., Fouateu, R.Y., Penaye, J., et al. U–Pb dating of plutonic rocks involved in the nappe tectonic in southern Cameroon: consequence for the Pan-African orogenic evolution of the central African fold belt. *Journal of African Earth Sciences*, 44(4-5) (2006), 479-493.

[10] Manguelle-Dicoum, E., Bokosah, A.S., and Kwende-Mbanwi, T.E. Geophysical evidence for a major Precambrian schist-granite boundary in southern Cameroon. *Tectonophysics*, 205(4) (1992), 437-446.

[11] Ndougsa-Mbarga, T., Manguelle-Dicoum, E., Tabod, C.T., et al. Modélisation d'anomalies gravimétriques dans la région de Mengueme-Akonolinga (Cameroun). *Science, Technology and Development*, 10 (2003) 67-74.

[12] Tadjou, J. M., Nouayou, R., Kamguia, J., et al. Gravity analysis of the boundary between the Congo craton and the pan-africal belt of Cameroon. *Austrian Journal of Earth Sciences*, 102(1) (2009).

[13] Gouet, D.H., Ndougsa-Mbarga, T., Meying, A., et al. Gold mineralization channels identification in the Tindikala-Boutou Area (Eastern-Cameroon) using geoelectrical (DC & IP) methods: A case study. 2013.

[14] Gouet, D.H., Meying, A., Assembe, S. P., et al. Clay minerals channels identification in the Tindikala-Boutou area (eastern-Cameroon) along the Kadey River using direct current (DC) method. *Journal of Geoscience and Environment Protection*, 3, (6) (2015), p. 123.

[15] Gazel, J. et Gérard, G. Carte géologique de reconnaissance du Cameroun au 1/500000: coupure Batouri-Est avec une notice explicative. Archives de la Direction des Mines et de la Géologie du Cameroun. Yaoundé, 1954.

[16] Cornacchia, M. et Dars, R. Un trait structural majeur du continent Africain; les lineaments centrafricains du Cameroun au Golfe d'Aden. *Bulletin de la Société géologique de France*, 7(1) (1983), 101-109.

[17] Ngako, F., Jegouzo, P., et Nzenti, J.-P. Le Cisaillement Centre Camerounais. Rôle structural et géodynamique dans l'orogenèse panafricaine. Comptes rendus de l'Académie des sciences. Série 2, Mécanique, Physique, Chimie, Sciences de l'univers, Sciences de la Terre, 313(4) (1991), 457-463.

[18] Penaye, J., Toteu, S.F., Van Schmus, W.R., et al. U-Pb and Sm-Nd preliminary geochronologic data on the Yaoundé series, Cameroon: re-interpretation of the granulitic rocks as the suture of a collision in the centrafrican belt. Comptes rendus de l'Académie des sciences. Série 2, *Mécanique, Physique, Chimie, Sciences de l'univers, Sciences de la Terre*, 317(6) (1993), 789-794.

[19] Mvondo, H., Denbrok, S.W.J., and Ondoa, J.M. Evidence for symmetric extension and exhumation of the Yaounde nappe (Pan-African fold belt, Cameroon). *Journal of African Earth Sciences*, 36(3) (2003) 215-231.

[20] Mvondo, H., Owona, S., Ondoa, J.M., et al. Tectonic evolution of the Yaoundé segment of the Neoproterozoic Central African Orogenic Belt in southern Cameroon. *Canadian Journal of Earth Sciences*, 44(4) (2007), 433-444.

[21] Olinga, J.B., Mpesse, J.E., Minyem, D., et al. The Awae Ayos strike-slip shear zones (southern Cameroon): Geometry, kinematics and significance in the late Pan-African tectonics. *Neues Jahrbuch für Geologie und Paläontologie-Abhandlungen*, (2010) 1-11.

[22] Gazel, J., Hourcq, V. et Nicklès, M. Carte géologique du Cameroun au 1/1.000. 000: notice explicative. Direction des mines et de la geologie du Cameroun, 1956.

[23] Augustin Didier, P.M., Théophile, N.M., Arsène, M., et al. New Geological and Structural Facts under the Lateritic Cover in Garga Sarali, Ndokayo (East Cameroon) Area, from Audiomagnetotellurics Soundings. *International Journal of Geophysics*, 2018, vol. 2018.

[24] Tchameni, R., Mezger, Klaus, Nsifa, N.E., et al. Crustal origin of Early Proterozoic syenites in the Congo craton (Ntem complex), South Cameroon. *Lithos*, 57(1) (2001), 23-42.

[25] Vicat, J.P. et Bilong, P. Esquisse géologique du Cameroun. Géosciences au Cameroun, 1(1998), 3-11.

[26] Poidevin, J.L. La tectonique Panafricaine à la bordure Nord du craton du Congo. L'orogenèse des oubanguides, 12th coll. Afr. Geol, 75, 1983.

[27] Trompette, Roland. Geology of western Gondwana (2000-500 Ma): Pan-Africa-Brasiliano aggregation of South America and Africa. 1994.

[28] Rolin, P. La zone de décrochements panafricains des Oubanguides en République Centrafricaine. Comptes rendus de l'Académie des sciences. Série 2. *Sciences de la terre et des planètes*, 320(1) (1995), 63-69.

[29] Toteu, S.F., Van Schmus, W.R., Penaye, J., et al. New U–Pb and Sm–Nd data from north-central Cameroon and its bearing on the pre-Pan African history of central Africa. *Precambrian Research*, 108(1-2) (2001), 45-73.

[30] Shandini, Y.N., Tadjou, J.M., Tabod, C.T., et al. Gravity Data Interpretation in the Northern Edge of the Congo Craton, South-Cameroon. *Anuário do Instituto de Geociências*, 33(1) (2010).

[31] Toteu, S.F., Van Schmus, W.R., Penaye, J., et al. U Pb and Sm N edvidence for Eburnian and Pan-African high-grade metamorphism in cratonic rocks of southern Cameroon. *Precambrian Research*, 67(3-4) (1994), 321-347.

[32] Pavlis, N., Kenyon, S., Factor, J., et al. Earth gravitational model 2008. In: SEG Technical Program Expanded Abstracts 2008. *Society of Exploration Geophysicists*, (2008) 761-763.

[33] Eyike, A. and Ebbing, J. Lithospheric structure of the West and Central African Rift System from regional three-dimensional gravity modelling. *South African Journal of Geology*, 118(3) (2015), 285-298.

[34] Eyike, A., Werner, S. C., Ebbing, Jörg, et al. On the use of global potential field models for regional interpretation of the West and Central African Rift System. *Tectonophysics*, 492(1-4) (2010), 25-39.

[35] Roest, W.R., Verhoef, J., and Pilkington, M. Magnetic interpretation using the 3-D analytic signal. *Geophysics*, 57(1) (1992), 116-125.

[36] Cordell, Lindrith. Gravimetric expression of graben faulting in Santa Fe Country and the Espanola Basin. In: New Mexico Geological Society Guidebook, *30th Field Conference*, New Mexico, (1979), 59-64.

[37] Cordell, L. and Grauch, V. J. S. Mapping basement magnetization zones from aeromagnetic data in the San Juan Basin, New Mexico. In: The utility of regional gravity and magnetic anomaly maps. *Society of Exploration Geophysicists*, (1985), 181-197.

[38] Blakely, Richard J. and Simpson, Robert W. Approximating edges of source bodies from magnetic or gravity anomalies. *Geophysics*, 51(7) (1986), 1494-1498.

[39] Grauch, V.J.S. and Hudson, M.R. Guides to understanding the aeromagnetic expression of faults in sedimentary basins: Lessons learned from the central Rio Grande rift, New Mexico. *Geosphere*, 3(6) (2007), 596-623.

[40] Philips JD. Processing and interpretation of aeromagnetic data for the Santa Cruz Basin-Pataphonia mountains area, South-Central Arizona. U.S. Geological Survey Open-file Report, Arizona, (1998) 02-98.